

Utah State University

DigitalCommons@USU

International Symposium on Hydraulic Structures

May 17th, 11:55 AM

Envelope Trajectory of Water Jet Issuing From a Thin Weir Obtained by Photogrammetry

Yvan Bercovitz

EDF R&D, yvan.bercovitz@edf.fr

William Barrey

Engineering School for Innovative Technologies, william.barrey@etu.univ-rouen.fr

Franck Lebert

EDF R&D, franck.lebert@edf.fr

Clément Buvat

EDF R&D, clement.buvat@edf.fr

Follow this and additional works at: <https://digitalcommons.usu.edu/ishs>

Recommended Citation

Bercovitz, Yvan (2018). Envelope Trajectory of Water Jet Issuing From a Thin Weir Obtained by Photogrammetry. Daniel Bung, Blake Tullis, 7th IAHR International Symposium on Hydraulic Structures, Aachen, Germany, 15-18 May. doi: 10.15142/T3793R (978-0-692-13277-7).

This Event is brought to you for free and open access by the Conferences and Events at DigitalCommons@USU. It has been accepted for inclusion in International Symposium on Hydraulic Structures by an authorized administrator of DigitalCommons@USU. For more information, please contact digitalcommons@usu.edu.



Envelope trajectory of water jet issuing from a thin weir obtained by photogrammetry

Y. Bercovitz¹, W. Barrey², F. Lebert¹, C. Buvat^{1,3}

¹EDF R&D Laboratoire National d'Hydraulique et d'Environnement, Chatou, France

²Engineering School for Innovative Technologies

³Saint Venant Laboratory for Hydraulics, Chatou, France

E-mail: yvan.bercovitz@edf.fr

Abstract: Today, to have a good command of the energy dissipation of a jet issuing from a weir, we need to improve our knowledge of the location of the impact. This laboratory experiment applied photogrammetry to determine the envelope trajectory of a water jet coming from a thin wall weir. The fall was about 9 meters, the weir was 1 meter wide, and the flow was up to 500 l/s. The trajectory of the jet was reconstituted in the three spatial dimensions using the PhotoScan software package developed by Agisoft. The exposure time for each picture was enough to make white water. Envelope trajectory was compared to classical expressions such as those of Scimeni (1937) or De Marchi (1928).

Keywords: Photogrammetry, jet, weir.

1. Introduction

The hydrodynamics of jets issuing from a weir is not yet well controlled. The approaches used in engineering assume flow to be monophasic, leading to overestimation of dynamic power and pressure at the impact point. Interaction between air and water along the jet leads to dissipation of energy. A better estimation of the forces involved could reduce the cost of protecting constructions against flooding, especially as safety regulations are currently becoming stricter.

To improve control of energy dissipation in jets issuing from a weir, we ran a series of trials on a new experimental set-up representing a 9 meters waterfall.

The present report continues our work using photogrammetry, improving estimation of jet trajectory so as to determine precisely the impact zone according to fall height and to correct optic effects for future Large Scale Particle Image Velocimetry (LS-PIV) applications.

Photogrammetry is an image processing procedure, reconstituting a scene in 3D from a series of photographs taken from different angles.

2. Trial conditions

2.1. General characteristics of the trial set-up

Table 1 shows the main characteristics:

Table 1. Main characteristics of the experimental set-up

Typology	Characteristics
Weir	Thin crest
Spill height	1 m
Basin length	2.9 m
Tranquillization method	Load loss + honeycombs
Max fall	9.5 m / slab – 15 m / cistern floor (4 m of water)
Q max	$0.5 \text{ m}^3 \cdot \text{s}^{-1} \cdot \text{m}^{-1}$
Flow control	Electromagnetic flowmeter + valves

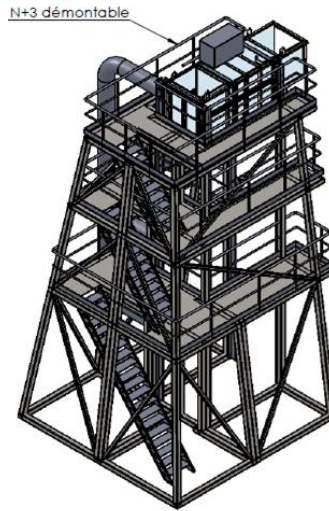


Figure 1. 3D representation of the experimental set-up



Figure 2. Spill at $0.220 \text{ m}^3 \cdot \text{s}^{-1}$

2.2. Reference frames

Dimensional processing of the measurements used the reference frame shown in Figure 3. For each trial, the coordinates of the measurement points were expressed in this frame.

Results were then rendered dimensionless and compared to trajectory expressions found in the literature. The frame here was that of Scimeni (1937) (Figure 4):

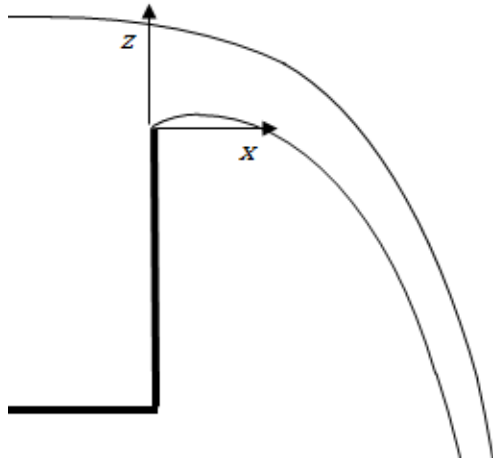


Figure 3. Dimensional frame

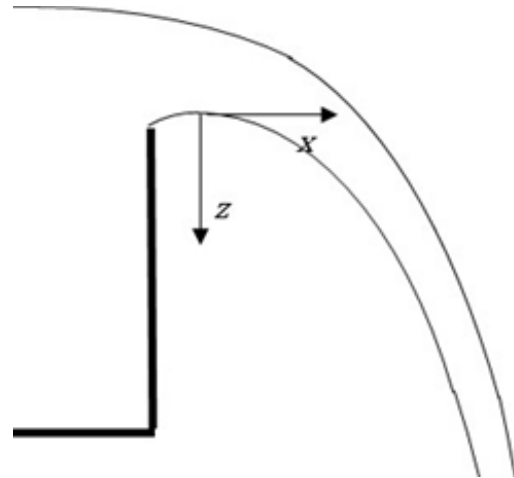


Figure 4. Scimeni's frame

In Scimeni's frame, the origin lies at the inflection point of the lower side of the jet. When the coordinates were rendered dimensionless by the head, the origin in the Scimeni frame represented a translation of the crest of $x/H = 0.2818$ and $z/H = 0.136$ (USCE 1970)

2.3. Reference scan

To express the point cloud in the dimensional frame (Figure 3), the cloud obtained on photogrammetry was superimposed on a reference cloud obtained by 3D scan laser. Table 2 shows the scan characteristics.

Table 2. 3D scan characteristics

Typology	Characteristics
Scanner reference	Faro Scan Laser
File name	Scan_laser_corrige.asc
Number of scan points	29,522,961

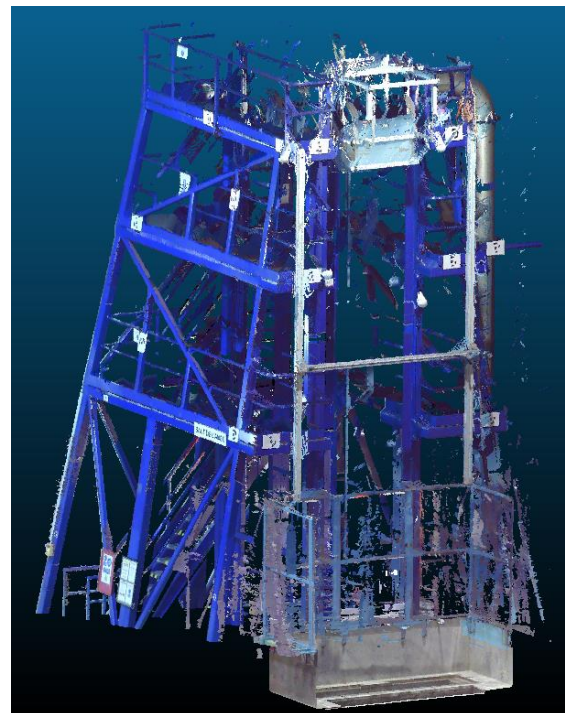


Figure 5. View of 3D scan

2.4. Study flowrates

Jet trajectory was measured for 8 flowrates. Table 3 shows height-flow correspondences.

Table 3. Study flowrates

Flowrate (m ³ .s ⁻¹)	Head over crest (m)
0.075	0.118
0.100	0.143
0.120	0.161
0.140	0.179
0.160	0.195
0.180	0.210
0.200	0.225
0.220	0.240

Head over crest was not measured, but calculated from Rehbock's formula (1929):

$$q = \mu \sqrt{2g} H^{3/2} \quad (1)$$

with:

$$\mu = \frac{2}{3} \left(0.605 + \frac{1}{1050H - 3} + 0.08 \frac{H}{p} \right) \quad (2)$$

where

q : linear flow (m³/s/m)

g : gravitational acceleration (m/s²)

H : head over crest (m)

p : crest height

μ : flow coefficient

2.5. Photogrammetry parameters

Table 4 shows the parameters in common to all photogrammetric measurements.

Table 4. Parameters in common to all photogrammetric measurements


Typology	Characteristics
Software	PhotoScan professional edition, version 1.2.6 ¹
Number of targets	16
Type of target	
Camera	Nikon D7100
Exposure parameters	
Iso sensitivity	160
Aperture	f/7.1 (f = focal length)
Pause time	3 s
Quality	RAW (except for 220 l/s in jpeg)

Figure 6 : Example of PhotoScan target

Table 5 shows the number of shots per trial.

Table 5. Number of shots per trial

Flowrate (m ³ .s ⁻¹)	Number of shots
0.075	49
0.100	51
0.120	57
0.140	56
0.160	45
0.180	46
0.200	56
0.220	44

¹ For use of PhotoScan, see **Error! Reference source not found.**

3. Data processing

The point clouds provided by PhotoScan were cleaned up using CloudCompare version 2.7.1, deleting points of the scene not corresponding to the jet (from (a) to (b) in **Error! Reference source not found.**), then manually deleting the edges of the jet to eliminate any edge effect (from (b) to (c) in **Error! Reference source not found.**).

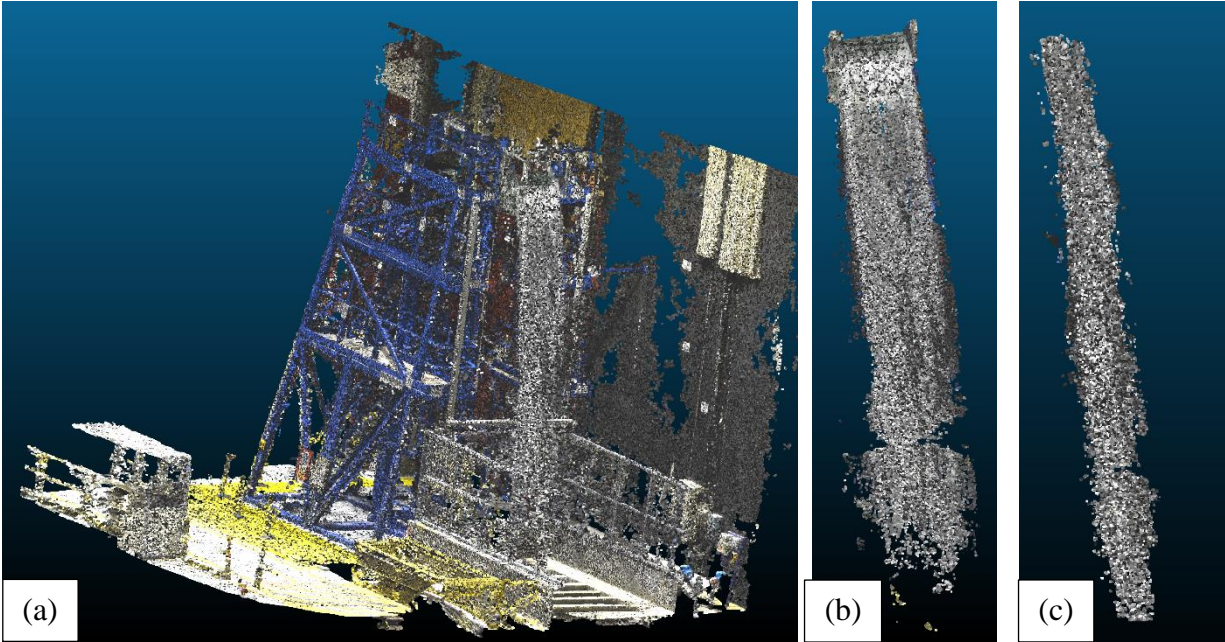


Figure 7. Example of cloud cleaning by CloudCompare: (a) complete scene, (b) extraction of jet, (c) extraction of central part of jet

Points were then projected onto the (x, z) plane, and rgb coloring was transformed into a grayscale using the following formula (Rec 709):

$$Gray = 0.2126 \times Red + 0.7152 \times Green + 0.0722 \times Blue \quad (3)$$

The point cloud was then statistically filtered for white intensity: a local χ^2 test selected points white enough to represent water. Finally, to avoid weighting one point cloud more than another, points were randomly deleted so that the maximal local intensity (number of points in a 2 cm radius disk) was the same in all clouds (7,341,022 pts/m²).

4. Analysis of results

After processing the point clouds, we estimated jet trajectory for each flowrate. NB: beyond 6 meters' fall, measurements were approximate, due to the transparent anti-spatter screens around the jet reception area.

4.1. Trajectory

In the Scimeni frame (Figure 4), for the lower side of the jet, the results were as follows, rendered dimensionless by the head over the crest (H).

According to De Marchi (1928):

$$\frac{z}{H} = 0.556 \left(\frac{x}{H} \right)^2 \quad (4)$$

According to Scimeni (1937):

$$\frac{z}{H} = \frac{1}{2} \left(\frac{x}{H} \right)^{1.85} \quad (5)$$

The trend plots take the following form:

$$\frac{z}{H} = -\alpha \left(\frac{x}{H} \right)^{\beta} + 0.375 \quad (6)$$

The trend plots are intended to express the trajectory of the center of the jet, which explains the 0.375 translation, corresponding to half of the height of the free surface with $x=0$ for a standard threshold, following Vischer and Hager (1999).

We also calculated two linear regressions for each point cloud: one after the first meter fall and one after 2 meters' fall. The resulting slopes allowed optical correction of the orthorectification required for LS-PIV processing. For the linear regressions, "a" stands for the slope coefficient and "b" for the y-intercept point. α, β, a and b are given for each flowrate; a and b are given for the linear regressions on the point clouds after 1 and 2 meters' fall.

For $0.075 \text{ m}^3 \cdot \text{s}^{-1} \cdot \text{m}^{-1}$ flow, results were compared to those of a trial carried out in October 2016 (**Error! Reference source not found.**). The SdA measurements correspond to the new data set, and JP measurements to the October 2016 data-set on a smaller test set-up, as used by Bercovitz et al. (2016). Bercovitz et al.'s (2016) slope corresponds to our first trajectory estimates.

In the SdA, the upper part of the jet was too transparent, and good quality measurements were not obtained before a fall of about 2.5 meters. The trend curve, however, was coherent with those of other trials (Fig. 9 and Table 6). In the new trial, the jet was slightly more downstream than in the JP measurements on the earlier set-up. The new measurements also gave a narrower jet, corresponding to a less well-developed jet state. These differences seemed to be related to turbulence intensity, which presumably was more intense in the plunging jet JP than in the SdA; this needs checking on further trials at constant flowrate, varying turbulence intensity above the weir.

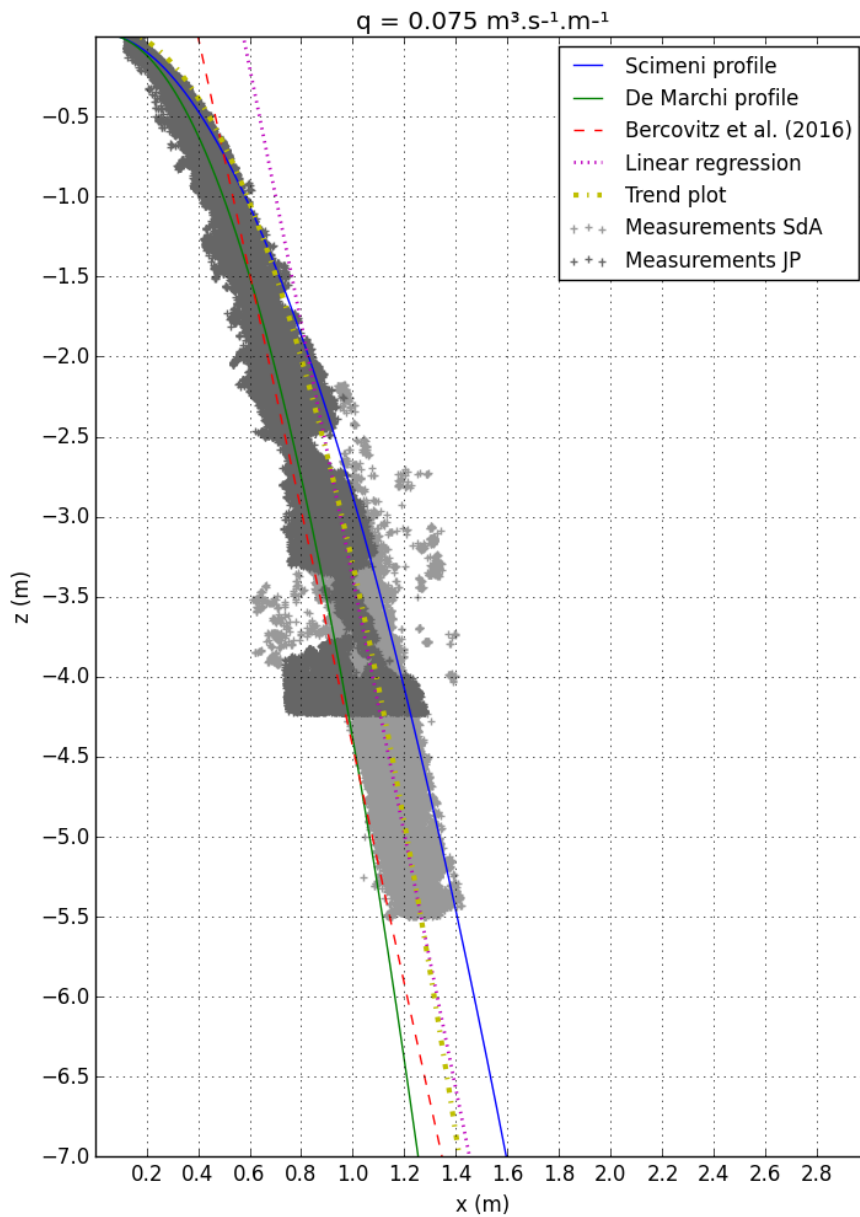


Figure 8. Trajectory for $0.075\text{m}^3\text{s}^{-1}\text{m}^{-1}$

Error! Reference source not found. shows trajectory measurements for flowrates between $0.075\text{ m}^3\cdot\text{s}^{-1}\cdot\text{m}^{-1}$ and $0.220\text{ m}^3\cdot\text{s}^{-1}\cdot\text{m}^{-1}$. Lengths are rendered dimensionless by the head over the crest.

At the foot of the fall, the maximum difference between curves was of the order of 2.5% of the fall height. The De Marchi profile tends to trace to lower trajectory of the jet, while the Scimeni profile is shifted too far downstream, in agreement with Bercovitz et al. (2016). Both of these curves are intended to correspond to the lower side of the jet. The general trend curve was obtained by applying the least squares method to all of the photogrammetric point clouds.

The general trend plot equation gave a good estimate of the trajectory of a jet issuing from a weir with a thin crest. Table 6 show trend curve and linear regression parameters.

In the trials, as of 5 meters' fall the measurement area was surrounded by transparent anti-splatter screens to prevent the working environment getting too wet. Also, the transparency of the basin impaired photogrammetric quality over the first meter of the fall. Trajectory measurements were therefore restricted to 1-5.5 meters' fall.

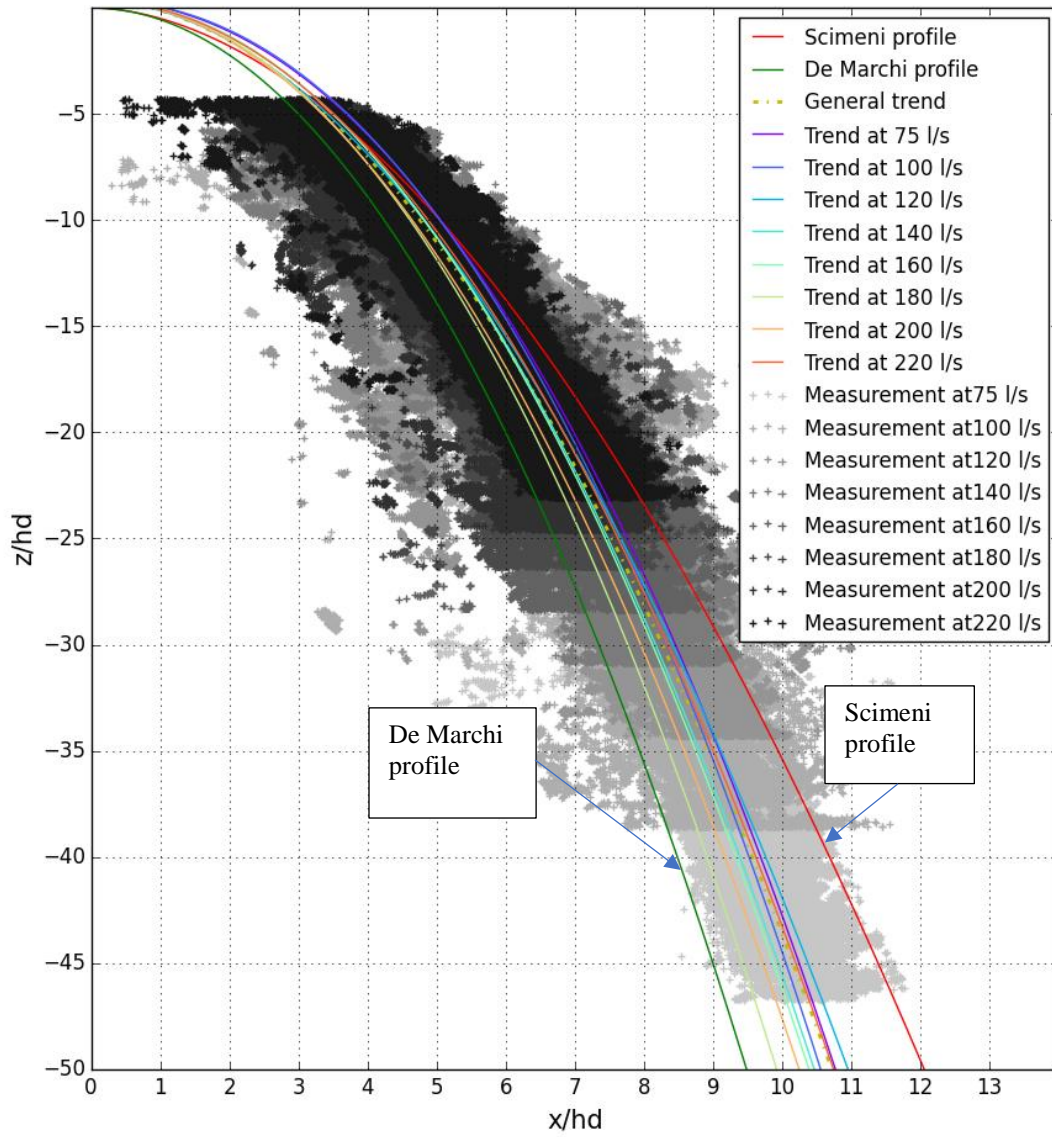


Figure 9. Dimensionless trajectories

Table 6. Trend plot and linear regression parameters

Flowrate (m ³ .s ⁻¹ .m ⁻¹)	Number of points (final cloud)	α	β	a (z<-1 m)	b (z<-1 m)	a (z<-2 m)	b (z<-2 m)
0.075	40 942	-0.35	2.09	-	-	-7.98	4.60
0.100	114 102	-0.32	2.14	-6.40	3.23	-7.81	5.17
0.120	104 919	-0.51	1.92	-5.41	2.62	-6.02	3.53
0.140	116 552	-0.42	2.04	-5.55	3.20	-5.73	3.39
0.160	120 310	-0.41	2.06	-5.36	3.96	-5.88	3.91
0.180	111 983	-0.44	2.07	-5.41	3.72	-5.88	3.89
0.200	103 051	-0.48	2.00	-5.05	3.08	-5.16	3.28
0.220	109 099	-0.44	2.00	-4.60	3.36	-5.09	3.78
General trend	820 958	-0.50	1.95				

5. Conclusion

Photogrammetry enabled precise estimation of mean jet trajectory in a 5.5 meter fall, with error estimated at 2.5%, enabling a simple analytic expression of the curve to be developed, in the Scimeni frame, for a linear flow range of 0.075 m³.s⁻¹.m⁻¹ to 0.220 m³.s⁻¹.m⁻¹:

$$\frac{z}{H} = -0.5 \left(\frac{x}{H} \right)^{1.95} + 0.375 \quad (7)$$

Initial developments have been undertaken to determine jet thickness and envelope, but the selection criteria for points in the raw cloud need refining, and measurement should be completed using other techniques, such as pressure distribution over the thickness of the jet.

Although transparent, the anti-spatter screens limit the height of fall that can be measured. It could be useful to supplement trials for the lower part of the jet with the screens removed, which could be done once the beams of the slab have been removed.

Tests could be made of the sensitivity of the trajectory to turbulence intensity.

6. References

- Bercovitz Y., Lebert F., Jodeau M., Buvat C., Violeau D., Pelaprat L. & Hajczak A. (2016) LS-PIV procedure applied to a plunging water jet issuing from an overflow nappe. *Proc. of the 4th IAHR Europe Congress*. July 27-29. Liège, Belgium.
- De Marchi G. (1928). Ricerche sperimentali sulle dighe tracimanti. *Annali dei lavori pubblici*. Il profile delle dighe sfioranti. *L'energia Elettrica*. Vol. 7. 14, 937-940.
- Rehbock T. (1929). Wassermessung mit scharfkantigen Ueberfaellen, *Zeitschrift VdI*, Vol. 73, 817-823.
- Scimeni E. (1937). Il profile delle dighe sfioranti. *L'energia Elettrica*. 14, 937-940.
- USCE. (1970). Hydraulic design criteria. Army Waterways Experiment Station. Vicksburg, MI.
- Vischer D.L. & Hager W.H. (1999). Dam Hydraulics. Wiley Series in Water Resources Engineering.